JOURNAL
OF THE AMERICAN CHEMICAL SOCIETY

VOLUME 106, NUMBER 20 OCTOBER 3, 1984

Formation and Reactivity of $Fe(CO)_4COOH^-$ in the Gas Phase. Implications for the $Fe(CO)_5$-Catalyzed Water-Gas Shift Reaction

Kelley R. Lane, Robert E. Lee, Larry Sallans, and Robert R. Squires*

Contribution from the Department of Chemistry, Purdue University, West Lafayette, Indiana 47907. *Received December 19, 1983*

Abstract: The iron carboxylic acid anion $Fe(CO)_4COOH^-$ has been generated in a flowing afterglow apparatus at 300 K from gas-phase ion-molecule reactions between hydroxide/water clusters, $HO(H_2O)_n^-$ ($n = 1–4$), and $Fe(CO)_5$. Reaction proceeds at or near the collision-limited rate for each of the OH^- hydrates and produces $Fe(CO)_4COOH^-$ as the sole ion product. In contrast, bare OH^- reacts with $Fe(CO)_5$ by addition and subsequent decarbonylation to yield $Fe(CO)_3OH^-$. Assignment of the iron hydroxycarbonyl structure to the product of the cluster ion reactions is based upon its observed hydrogen–deuterium exchange with deuterated carboxylic acids plus the nonoccurrence of binary switching reactions with highly polar neutrals such as might be expected if it were an electrostatically bound cluster ion. Estimates of $\Delta H_f[Fe(CO)_4COOH^-] \leq -257$ kcal/mol and $D°[Fe(CO)_5–OH^-] \geq 50$ kcal/mol are derived from the occurrence of reaction between $Fe(CO)_5$ and $HO(H_2O)_4^-$. $^{18}O/^{16}O$ scrambling does not occur when either bare $^{18}OH^-$ or $^{18}OH(H_2{}^{18}O)_n^-$ ions react with $Fe(CO)_5$, thereby indicating either irreversible hydroxide addition and/or a substantial barrier to intramolecular proton transfer within the iron carboxylic acid. The results of these studies are discussed in terms of the postulated role of $Fe(CO)_4COOH^-$ in the $Fe(CO)_5$-catalyzed water-gas shift reaction.

Homogeneous catalysis of the water-gas shift reaction (WGSR) by transition–metal carbonyls has received considerable attention since the first examples were reported some 50 years ago.[1-10] While good progress in our understanding of these catalytic cycles has been achieved, certain mechanistic details have remained

Scheme I

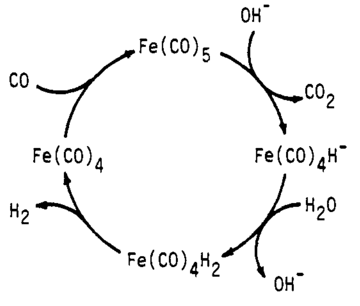

NET: $H_2O + CO \longrightarrow H_2 + CO_2$

---

(1) (a) Hieber, W.; Leutert, F. *Z. Anorg. Allg. Chem.* **1932**, *204*, 145–150. (b) Hieber, W.; Becker, E. *Chem. Ber.* **1930**, *63*, 1405–1407. (c) Hieber, W.; Abeck, W.; Platzer, H. K. *Z. Anorg. Allg. Chem.* **1955**, *280*, 241–251. (d) Hieber, W.; Rieger, K. *Ibid.* **1959**, *300*, 288–294, 295–303, 304–310.

(2) Reppe, J. W.; Reindl, E. *Liebigs Ann. Chem.* **1953**, *582*, 121–124.

(3) (a) Laine, R. M.; Rinker, R. G.; Ford, P. C. *J. Am. Chem. Soc.* **1977**, *99*, 252–253. (b) Ungermann, C.; Landis, V.; Moya, S. A.; Cohen, H.; Walker, H.; Pearson, R. G.; Rinker, R. G.; Ford, P. C. *Ibid.* **1979**, *101*, 5922–5929. (c) Ford, P. C.; Rinker, R. G.; Ungermann, C.; Laine, R. M.; Landis, V.; Moya, S. A. *Ibid.* **1978**, *100*, 4595–4597. (d) Ford, P. C.; Rinker, R. G.; Laine, R. M.; Ungermann, C.; Landis, V.; Moya, S. A. *Adv. Chem. Ser.* **1979**, *No. 173*, 81–93. (e) Ford, P. C.; Yarrow, P.; Cohen, H., *ACS Symp. Ser.* **1981**, *No. 152*, 95–105. (f) Ford, P. C. *Acc. Chem. Res.* **1981**, *14*, 31–37.

(4) (a) Kang, H.; Mauldin, C. H.; Cole, T.; Slegeir, W.; Cann, K.; Pettit, R. *J. Am. Chem. Soc.* **1977**, *99*, 8323–8325. (b) Pettit, R.; Cann, K.; Cole, T.; Maneden, C.; Slegeir, W., *Adv. Chem. Ser.* **1979**, No. 173, 121–130. (c) Grice, N.; Kao, S. C.; Pettit, R. *J. Am. Chem. Soc.* **1979**, *101*, 1623–1628.

(5) (a) King, R. B.; Frazier, C. C.; Hanes, R. M.; King, A. D. *J. Am. Chem. Soc.* **1978**, *100*, 2925–2927. (b) King, A. D.; King, R. B.; Yang, D. B. *Ibid.* **1980**, *102*, 1028–1032. (c) King, R. B.; King, A. D., Jr.; Yang, D. B. *ACS Symp. Ser.* **1979**, *No. 152*, 123–132. (d) Frazier, C. C.; Hanes, R. B.; King, A. D.; King, R. B. *Adv. Chem. Ser.* **1979**, *No. 173*, 94–105.

(6) (a) Cheng, C. H.; Hendricksen, D. E.; Eisenberg, R. *J. Am. Chem. Soc.* **1977**, *99*, 2791–2792. (b) Cheng, C. H.; Eisenberg, R. *Ibid.* **1978**, *100*, 5968–5970. (c) Baker, E. C.; Hendricksen, D. E.; Eisenberg, R. *Ibid.* **1980**, *102*, 1020–1027. (d) Kubiak, C. P.; Woodcock, C.; Eisenberg, R. *Inorg. Chem.* **1982**, *21*, 2119–2129. (e) Kubiak, C. P.; Eisenberg, R. *J. Am. Chem. Soc.* **1980**, *102*, 3637–3638. (f) Kullberg, M. L.; Kubiak, C. P. *J. C-1 Mol. Chem.*, submitted.

(7) (a) Darensbourg, D. J.; Froelich, J. A. *J. Am. Chem. Soc.* **1977**, *99*, 5940–5946, 4726–4729. (b) Darensbourg, D. J.; Darensbourg, M. Y.; Burch, R. R.; Froelich, J. A.; Incorvia, M. J. *Adv. Chem. Ser.* **1979**, *No. 173*, 106–120. (c) Darensbourg, D. J.; Rokicki, A. *ACS Symp. Ser.* **1981**, *No. 152*, 107–121 and references cited therein. (d) Darensbourg, D. J.; Rokicki, A. *Organometallics* **1982**, *1*, 1685–1693 and references cited therein.

(8) (a) Slegeir, W. A. R.; Sapienza, R. S.; Easterling, B. *ACS Symp. Ser.* **1981**, No. 152, 325–343. (b) Slegeir, W. A. R.; Sapienza, R. S.; Rayford, R.; Lam, L. *Organometallics* **1982**, *1*, 1728–1730.

(9) (a) Thomson, W. J.; Laine, R. M. *ACS Symp. Ser.* **1981**, No. 152, 133–145. (b) Laine, R. M. *J. Am. Chem. Soc.* **1978**, *100*, 6451–6454.

0002-7863/84/1506-5767$01.50/0

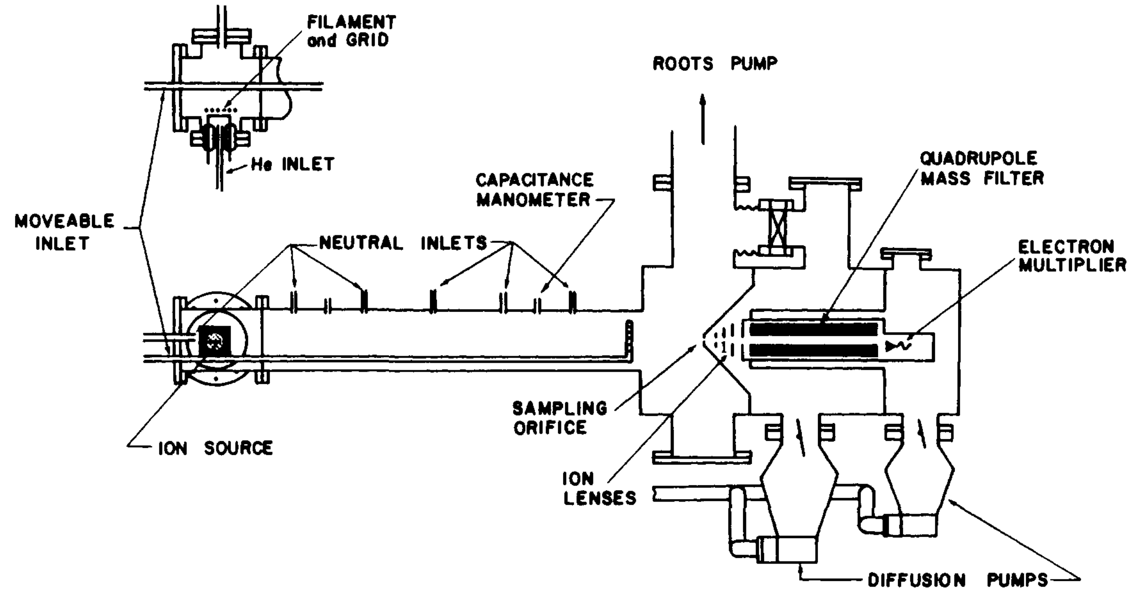

Figure 1. Flowing afterglow apparatus.

unclarified largely due to difficulties in identifying and characterizing the transient intermediate species which are postulated for many of the key steps. For example, a recent investigation of the kinetics of the WGSR catalyzed by $Fe(CO)_5$ in alkaline solution[11] (Scheme I) questioned earlier proposals[4] regarding the mode of decarboxylation of the metallocarboxylic acid **1** which is commonly believed to be the first formed intermediate in the catalytic cycle[4] (eq 1). Slight curvature in the pH dependence

$$\mathrm{Fe(CO)_5 + OH^- \rightarrow \underset{\mathbf{1}}{[(CO)_4FeCO_2H^-]} \rightarrow (CO)_4FeH^- + CO_2} \qquad (1)$$

of the rate of reation 1 led to the suggestion[11] that CO_2 loss proceeds via dianion **2** (eq 2) rather than directly from the iron carboxylic acid **1**. While similar conclusions have been reached

$$\mathrm{\underset{\mathbf{1}}{[(CO)_4FeCO_2H^-]} \xrightarrow{base} \underset{\mathbf{2}}{[(CO)_4FeCO_2^{2-}]} \xrightarrow{-CO_2} [(CO)_4Fe^{2-}] \xrightarrow{H^+} (CO)_4FeH^-} \qquad (2)$$

for related anionic and neutral metallocarboxylic acids.[7d,12] no clear trends in the general behavior of such complexes with respect to decarboxylation have been established.[13]

In the course of our studies of gas-phase transition-metal ion chemistry using the flowing afterglow method, we have recently generated the iron carboxylic acid **1** as well as several other examples of metallocarboxylic acid monoanions in the gas phase.[14] We report here the full details of our investigations of the properties and reactivity of this interesting metal ion complex as they relate to its proposed role in the $Fe(CO)_5$-catalyzed WGSR.

Experimental Section

Our experiments were carried out in a flowing afterglow (FA) apparatus[15] which was recently completed in our laboratories at Purdue. A simplified schematic of the FA is shown in Figure 1. Ions are produced by electron impact on neutral precursor gases added near a thorium oxide coated iridium filament and accelerating grid located in the upstream ionization region. A fast flow (100–250 STP $cm^3 s^{-1}$) of purified helium buffer gas also enters the instrument at this point and carries the plasma the length of a 1 m × 7.3 cm i.d. stainless steel flow reactor. The bulk flow velocity ($\sim$9100 cm s^{-1}) and flow tube pressure (0.1–0.9 torr) are maintained by a Tylan mass flow controller in combination with a 7550 L s^{-1} Roots blower which is housed in a soundproof enclosure adjacent to the instrument. Rapid thermalization of the ions and attainment of a well-defined laminar flow profile are achieved within the first upstream quarter of the flow tube. Multistep ion–molecule reaction sequences are executed by the introduction of neutral reactant gases into the ion stream through any of six fixed inlets positioned at regular intervals along the length of the reaction region or through a moveable neutral injector. The steady-state ion composition in the reactor is continuously monitored by an Extranuclear Laboratories, Inc. quadrupole mass filter located behind a 0.5-mm molybdenum sampling orifice which is mounted on a stainless steel nose cone. Either positive or negative ions may be sampled by appropriate choice of the polarities of voltages applied to the ion lenses mounted in front of the mass filter. Following mass selection, the ions are detected by a Ceratron-E electron multiplier. The detection region is maintained at a pressure of 10^{-6}–10^{-7} torr by differential pumping with two oil diffusion pumps. The data system for the FA incorporates a Digital Equipment Corporation LSI 11/23 minicomputer for mass spectrometer scan control and detector pulse counting as well as data display, storage, and analysis. The entire combination provides a mass range of 1–500 amu with an optimal resolution of 1200 at 131 amu. Mass discrimination is normally minimized by operating at as low a setting of the ion lenses and resolution controls as is practical.

A few of the experiments described here were carried out with our newly developed flowing afterglow-triple quadrupole. A preliminary account of the design and operation of this instrument has been submitted.[16] Briefly, the single-stage mass filter of the FA is replaced with a triple quadrupole analyzer (Finnigan-MAT TSQ)[17] which consists of three coaxially aligned quadrupole assemblies and an electron multiplier. The first and third quadrupoles are conventional mass analyzers; the second quadrupole is a focusing collision cell in which collision-induced dissociation (CID) of ions takes place against a relatively high-background pressure of argon (ca. 10^{-3} torr). In the daughter ion scanning mode employed here the first quadrupole is set to select a particular ion from the flow reactor while the third quadrupole is scanned, thereby providing a mass spectrum of the fragment ions produced by CID in the central quadrupole.

Bimolecular rate coefficients and ion product distributions are determined in the FA by standard methods which are described in detail

---

(10) (a) Yoshida, T.; Okano, T.; Otsuka, S. *ACS Symp. Ser.* **1981**, *No. 152*, 79–93. (b) Yoshida, T.; Ueda, Y.; Otsuka, S. *J. Am. Chem. Soc.* **1978**, *100*, 5968–5970. (c) Yoshida, T.; Thorn, D. L.; Okano, T.; Ibers, J. A.; Otsuka, S. *Ibid* **1979**, *101*, 4212–4221.

(11) Pearson, R. G.; Mauermann, H. *J. Am. Chem. Soc.* **1982**, *104*, 500–504.

(12) (a) Darensbourg, D. J.; Froelich, J. A. *Inorg. Chem.* **1978**, *17*, 3300–3304. (b) Bercaw, J. E.; Goh, L.; Halpern, J. *J. Am. Chem. Soc.* **1972**, *94*, 6534–6536.

(13) (a) Gibson, D. H.; Owens, K.; Ong, T. S. *J. Am. Chem. Soc.* **1984**, *106*, 1125–1126 and references cited therein. (b) Atton, J. G.; Kane-Maguire, L. A. P. *J. Organomet. Chem.* **1983**, *246*, C23–C26. (c) Barrientos-Penna, C. F.; Gilchrist, A. B.; Sutton, D. *Organometallics* **1983**, *2*, 1265–1266. (d) Sweet, J. R.; Graham, W. A. G. *Ibid.* **1982**, *1*, 982–986.

(14) Lane, K. R.; Sallans, L.; Squires, R. R. *Inorg. Chem.* **1984**, *23*, 1999–2000.

(15) (a) Ferguson, E. E.; Fehsenfeld, F. C.; Schmeltekopt, A. *Adv. At. Mol. Phys.* **1969**, *5*, 1–56. (b) Smith, D.; Adams, N. C. In "Gas Phase Ion Chemistry"; Bowers, M. T., Ed.; Academic Press: New York, 1979; Chapter 1. (c) DePuy, C. H.; Bierbaum, V. M. *Acc. Chem. Res.* **1981**, *14*, 146–153.

(16) Squires, R. R.; Lane, K. R.; Lee, R. E.; wright, L. G.; Wood, K. V.; Cooks, R. G., submitted for publication in *J. Am. Chem. Soc.*

(17) Slayback, J. R. B.; Story, M. S. *Ind. Res. Dev.* **1981**, 129.

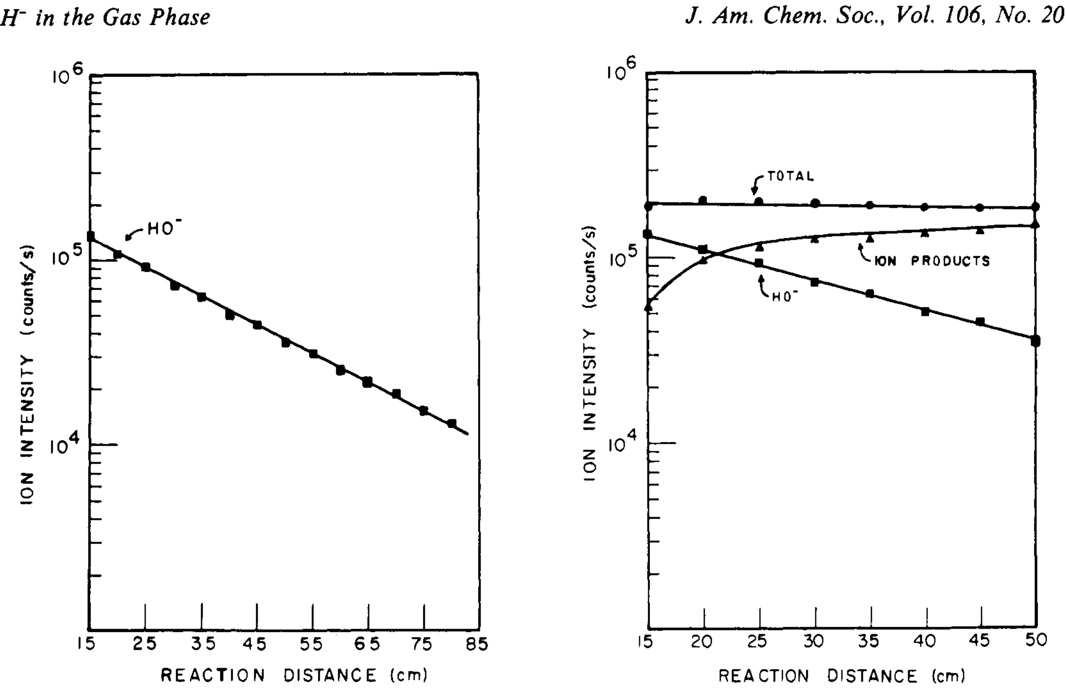

Figure 2. Kinetic data for the reaction $OH^- + Fe(CO)_5 \rightarrow Fe(CO)_3OH^- + 2CO$. Helium flow = 232 STP $cm^3\ s^{-1}$; total pressure = 0.500 torr; $Fe(CO)_5$ flow = 3.7×10^{-3} STP $cm^3\ s^{-1}$; $T = 296 \pm 2$ K; $k = 2.0 \times 10^{-9}\ cm^3\ molecule^{-1}\ s^{-1}$.

elsewhere.[15,18] Briefly, ion–molecule reactions such as eq 3 are carried out under pseudo-first-order conditions. Equation 4 is the standard

$$OH^- + Fe(CO)_5 \xrightarrow{k^{II}} Fe(CO)_3OH^- + 2CO \qquad (3)$$

expression for the binary rate coefficient, k^{II}, where z is the reaction distance (distance between the neutral inlet and detector; corrected for inlet end effects), $\bar{v}$ is the bulk flow velocity, and $\alpha = 1.6$ is a factor relating the flow velocity to the average transport velocity of the ions.[15]

$$k^{II} = -\frac{d(\ln [OH^-])}{dz}\frac{\alpha\bar{v}}{[Fe(CO)_5]} \qquad (4)$$

Incorporation of all experimentally determined parameters into eq 4 and collection of constants give eq 5. Ion abundances are monitored as a

$$k^{II}(cm^3\ molecule^{-1}\ s^{-1}) = -\frac{d(\log [OH^-])}{dz} \times \left[\frac{F_{He}^2\left[\frac{STP\ cm^3}{s}\right]^2 T(K)}{P_{He}^2(torr^2)F_{Fe(CO)_5}\left[\frac{STP\ cm^3}{s}\right]}\right] \times 7.53 \times 10^{-18} \qquad (5)$$

function of either the neutral inlet position at fixed neutral flow rate or neutral flow rate at fixed inlet position ($F(Fe(CO)_5)$ and z are transposed in eq 5). Neutral flow rates are measured by diverting the flow into a calibrated volume and monitoring the pressure increase with time as measured by a capacitance manometer. Plots of the log of the reactant ion intensity vs. reaction distance or substrate flow rate provide a binary rate coefficient with an estimated accuracy of ±20%. Figure 2 shows a typical plot of data for reaction 3. Combining the slope from Figure 2 (−0.01558) with F_{He} = 232 STP $cm^3\ s^{-1}$, P_{He} = 0.500 torr, $F(Fe(CO)_5)$ = 3.7×10^{-3} STP $cm^3\ s^{-1}$, and T = 296 K gives a rate constant of $2.0 \times 10^{-9}\ cm^3\ molecule^{-1}\ s^{-1}$. Product branching ratios are determined either by extrapolating normalized product ion abundances to zero reaction time (distance) or zero neutral flow rate or from the slope of a plot of relative product ion intensity vs. relative conversion of reactant ion.[18] Measurements of the rate and product ion branching ratio for the reaction of He^+ with N_2 give average values from four determinations of $1.5 \pm 0.5 \times 10^{-9}\ cm^3\ molecule^{-1}\ s^{-1}$ and 56% N^+/44% N_2^+, respectively, in excellent agreement with previous determinations from other laboratories.[19]

Hydroxide ion was generated in the ionization region from dissociative electron capture by N_2O followed by hydrogen atom abstraction from CH_4. OD^- and $^{18}OH^-$ were formed by electron impact on D_2O and $H_2{}^{18}O$, respectively. The hydrated hydroxide ions $HO(H_2O)_n^-$ (n = 1–4) and labeled analogues $DO(D_2O)_n^-$ and $H^{18}O\ (H_2{}^{18}O)_n^-$ were each produced by adding variable flows of water vapor near the ion source filament in combination with lesser flows of N_2O and CH_4. Relatively rapid termolecular association reactions at 0.4-torr reactor pressure establish a kinetic mixture of cluster ions prior to the reaction region.[20] A significant increase in the rate and extent of OH^- hydration could be induced by adding moderate flows (~0.01 STP $cm^3\ s^{-1}$) of tetrahydrofuran (THF) to the system at the furthest upstream inlet. While this phenomenon is not completely understood at present, it is most likely due to a specific facilitation of the hydroxide–water clustering rate from more effective three-body stabilization by the large polyatomic neutral THF.

Gas purities were as follows: helium (99.995%), methane (99.0%), and nitrous oxide (99.0%). $H_2{}^{18}O$ (99 mol % ^{18}O), D_2O (99.8 mol % D), CH_3COOD (98 mol % D), and all other reagents were obtained from commerical sources and were subjected to multiple freeze–pump–thaw cycles prior to use to remove noncondensable impurities.

Results and Discussion

We have examined the gas-phase reactions of a wide variety of anionic nucleophiles with $Fe(CO)_5$, $Cr(CO)_6$, and other transition-metal carbonyls.[21] As is typical for strongly basic anions, hydroxide undergoes a rapid reaction with $Fe(CO)_5$ to produce an iron tricarbonyl adduct species, $Fe(CO)_3OH^-$, as the exclusive product (eq 3). Comparison of the measured bimolecular rate coefficient ($2.1 \pm 0.2 \times 10^{-9}\ cm^3\ molecule^{-1}\ s^{-1}$) with the corresponding Langevin collision rate constant[22] ($3.1 \times 10^{-9}\ cm^3\ molecule^{-1}\ s^{-1}$) indicates that formation of $Fe(CO)_3OH^-$ occurs on nearly every encounter. Neither the rate nor outcome of reaction 3 exhibits any pressure dependence over the range 0.2–0.8 torr. The efficiency of the decarbonylation reaction (3) is further illustrated by the lack of $^{18}O/^{16}O$ exchange found when $^{18}OH^-$ is the reactant ion (eq 6). Here, reversible hydroxide addition

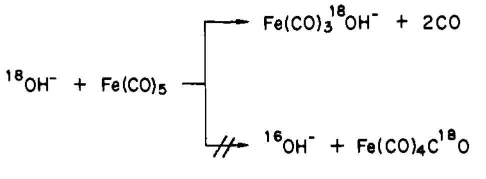

(6)

---

(18) (a) Squires, R. R.; Bierbaum, V. M.; Grabowski, J. J.; DePuy, C. H. *J. Am. Chem. Soc.* **1983**, *105*, 5185–5192. (b) Smith, D.; Adams, N. G. *J. Phys. B* **1976**, *9*, 1439–1451. (c) Anderson, D. R.; Bierbaum, V. M.; DePuy, C. H. *J. Am. Chem. Soc.* **1983**, *105*, 4244–4248.

(19) Albritton, D. L. *At. Data Nucl. Data Tables* **1978**, *22*, 1–101.

(20) Fehsenfeld, F. C.; Ferguson, E. E., *J. Chem. Phys.* **1974**, *61*, 3181–3193.

(21) Lane, K. R.; Sallans, L.; Squires, R. R., manuscript in preparation. For an earlier report on reactions between gaseous anions and $Fe(CO)_5$ see: Foster, M. S.; Beauchamp, J. L. *J. Am. Chem. Soc.* **1975**, *97*, 4808–4814.

(22) Su, T.; Bowers, M. T. In "Gas Phase Ion Chemistry", Bowers, M. T., Ed.; Academic Press: New York, **1979**; Chapter 3.

Table I. Kinetic Data for Reactions of Iron Pentacarbonyl with $DO(D_2O)_n^-$ (Eq 8) at 300 K

n	k_{obsd}[a]	reaction efficiency[b]
1	2.3	1.0
2	2.1	1.1
3	1.8	1.1
4	0.97	0.64

[a] In units of 10^{-9} cm^3 molecule^{-1} s^{-1}. [b] Reaction efficiency = $k_{obsd}/k_{Langevin}$, ref 22.

to $Fe(CO)_5$ with accompanying intramolecular proton transfer would, in principle, be exposed either by appearance of $^{16}OH^-$ as a primary reaction product or by production of $Fe(CO)_3{}^{16}OH^-$ through its subsequent fast reaction with iron pentacarbonyl. Oxygen exchanges of this type have been observed previously by DePuy and co-workers[23] in reactions of $^{18}OH^-$ with CO_2, CH_2O, SO_2, N_2O, and oxetane, however no such scrambling is evident for $Fe(CO)_5$. Presuming that hydroxide reacts with $Fe(CO)_5$ by initial attachment to one of the CO ligands[24] (vide infra), the apparent lack of $^{18}O/^{16}O$ exchange suggests that either addition is irreversible and/or the barrier to the required intramolecular proton transfer exceeds that for CO expulsion.[25]

At elevated $Fe(CO)_5$ flow rates, we observe the appearance of dinuclear condensation ions in which 0, 1, and 2 CO ligands have been expelled (eq 7). Similar diiron cluster anions have been observed previously by ion cyclotron resonance spectrometry (ICR).[26]

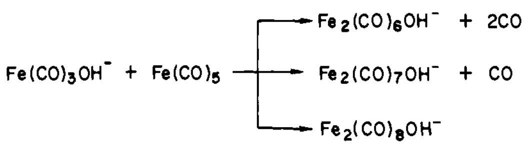

$$Fe(CO)_3OH^- + Fe(CO)_5 \longrightarrow \begin{cases} Fe_2(CO)_6OH^- + 2CO \\ Fe_2(CO)_7OH^- + CO \\ Fe_2(CO)_8OH^- \end{cases} \quad (7)$$

The presence of just a single solvent water molecule alters the course of the reaction between hydroxide and $Fe(CO)_5$ in a striking fashion.[27] The hydrated deuteroxide ions $OD(D_2O)_n^-$, n = 1, 2, 3, 4, *all* react with $Fe(CO)_5$ to yield exclusively the ion product **3** (m/z 214) (eq 8). Reaction is rapid for each of the solvated

$$OD(D_2O)_n^- + Fe(CO)_5 \rightarrow \underset{\mathbf{3}}{Fe(CO)_5OD^-} + nD_2O \quad (8)$$

$$n = 1, 2, 3, 4$$

ion reactants as indicated by the data summarized in Table I. Care was taken to measure the reaction rates for each hydrate and monitor the ion abundances over a range of conditions of D_2O flow rate and clustering reaction time in order to ensure that their observed decays were due only to reaction with $Fe(CO)_5$ and not simply a result of precursor ion depletion. No further reactions of **3** with either $Fe(CO)_5$ or D_2O are observed nor do any new iron-containing products appear at elevated reactor pressures (up to 0.8 torr).

When the labeled hydrates, $^{18}OH(H_2{}^{18}O)_n^-$ (n = 1–3), serve as the reactant ions, no more than one ^{18}O appears in the product of reaction 8. Therefore, as with the bare ion reaction, hydroxide addition to $Fe(CO)_5$ is either irreversible under these conditions and/or the requisite intramolecular proton transfer does not occur—even with up to three water molecules present within the initial collision complex.

Scheme II

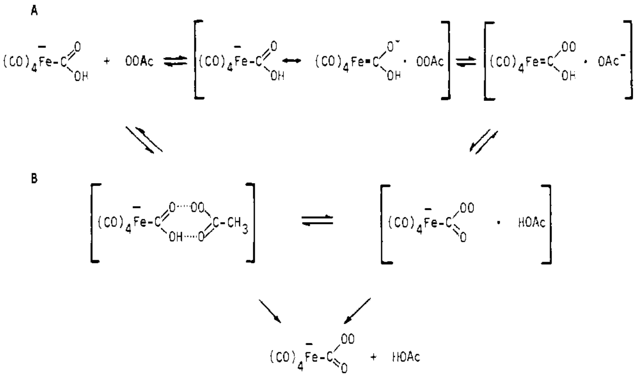

Our assignment of the iron carboxylic acid structure **1** to the product of reaction 8 is based on several lines of chemical evidence and thermodynamic reasoning. We rule out an electrostatically bound ion–molecule complex such as **4** in favor of a structure involving stronger covalent bonding to OH^-. This is a nontrivial point since $Fe(CO)_5$ possesses a relatively large polarizability (28 Å^3),[28] and the corresponding ion-induced dipole attraction energies may become substantial for $HO^-/Fe(CO)_5$ separation distances of a few angstroms.[29] However, since the reaction between bare OH^- and $Fe(CO)_5$ (eq 3) results in expulsion of two CO ligands and the hydrated ions all react at or near the collision rate with no solvent retention by the product (eq 8), we believe that strong covalent bonding interactions must be operative.[30] Indeed, the occurrence of reaction 8 for n = 4 permits an estimate of a lower limit to $D°[Fe(CO)_5\text{–}OD^-]$ of ≥50 kcal/mol.[31] Furthermore, neutral switching type reactions such as might be expected for an electrostatically bound cluster ion,[30] **4**, are *not* observed when **3** is allowed to react with neutral substrates possessing large permanent dipole moments such as CH_3NO_2 (μ_D = 3.46 D).[32] Structure **5**, which represents the isomeric formate anion,[7d] is also contraindicated by our observation that **3** undergoes H/D exchange in the presence of simple carboxylic acids and H_2S, as does its protonated analogue in the presence of CH_3COOD (eq 9–11).

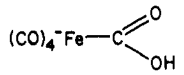

1

$[Fe(CO)_5 \cdots OH^-]$

4

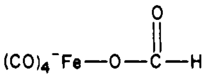

$$(CO)_4{}^-Fe\text{—}O\text{—}\overset{\overset{\displaystyle O}{\|}}{C}\text{—}H$$

5

$$(CO)_4FeCO_2D^- + HCO_2H \rightarrow (CO)_4FeCO_2H^- + HCO_2D \quad (9)$$

$$(CO)_4FeCO_2D^- + H_2S \rightarrow (CO)_4FeCO_2H^- + HSD \quad (10)$$

$$(CO)_4FeCO_2H^- + CH_3CO_2D \rightarrow (CO)_4FeCO_2D^- + CH_3CO_2H \quad (11)$$

It is unlikely that the formyl proton in structure **5** would be subject

---

[23] (a) DePuy, C. H. In "Ionic Processes in the Gas Phase"; Ferriera, M. A. A., Ed.; Reidel: Dordrecht, 1984. (b) Nibbering, N. M. M. *Recl. Trav. Chim. Pays-Bas* **1981**, *100*, 297–306.

[24] Collman, J. P.; Hegedus, L. S. "Principles and Applications of Organotransition Metal Chemistry"; University Science Books; Mill Valley, CA 1980.

[25] $Fe(CO)_5$ also resists oxygen exchange in alkaline solution, cf.: Darensbourg, D. J.; Darensbourg, M. Y.; Walker, N.; Froelich, J. A.; Barros, H. L. C. *Inorg. Chem.* **1979**, *18*, 1401–1402.

[26] (a) Wronka, J.; Ridge, D. P. *J. Am. Chem. Soc.* **1984**, *106*, 67–71. (b) Dunbar, R. C.; Ennever, J. F.; Fackler, J. P. *Inorg. Chem.* **1973**, *12*, 2734–2736.

[27] Other effects of ion solvation on gas-phase proton transfers, substitutions, and Michael additions have been described, c.f.; Raksit, A. B.; Bohme, D. K. *Can. J. Chem.* **1983**, *61*, 1683–1689 and references cited therein. Bartmess, J. E. *J. Am. Chem. Soc.* **1980**, *102*, 2483–2484. Caldwell, G.; Rosenboom, M. D.; Kiplinger, J. P.; Bartmess, J. E. *Ibid.* **1984**, *106*, 809–810.

[28] Dorfman, Y. G., *Z. Fiz. Khim.* **1963**, *37*, 2496–2503.

[29] Using a simple ion-induced dipole potential $V(r) = -\alpha q/r^4$ where α is the molecular polarizability and q is the ionic charge gives interaction energies (ignoring repulsion) of ~7.4, ~18.1, and ~57.3 kcal/mol for r = 5, 4, and 3 Å, respectively.

[30] Bohme, D. K. In "Ionic Processes in the Gas Phase"; Ferreira, M. A. A., Ed., Reidel: Dordrecht, 1984.

[31] Based upon data from: Payzant, J. D.; Yamdagni, R.; Kebarle, P. *Can. J. Chem.* **1971**, *49*, 3308–3314. Arshadi, M.; Kebarle, P. *J. Phys. Chem.* **1970**, *74*, 1483–1485. $D[4(H_2O)\text{–}OH^-]$ = 72.2 kcal/mol and an estimated entropy contribution of 73.9 eu for reaction 8, n = 4.

[32] McClellan, A. L. "Table of Experimental Dipole Moments"; Rahara Enterprises: El Cerrito, CA, 1979; Vol. 2.

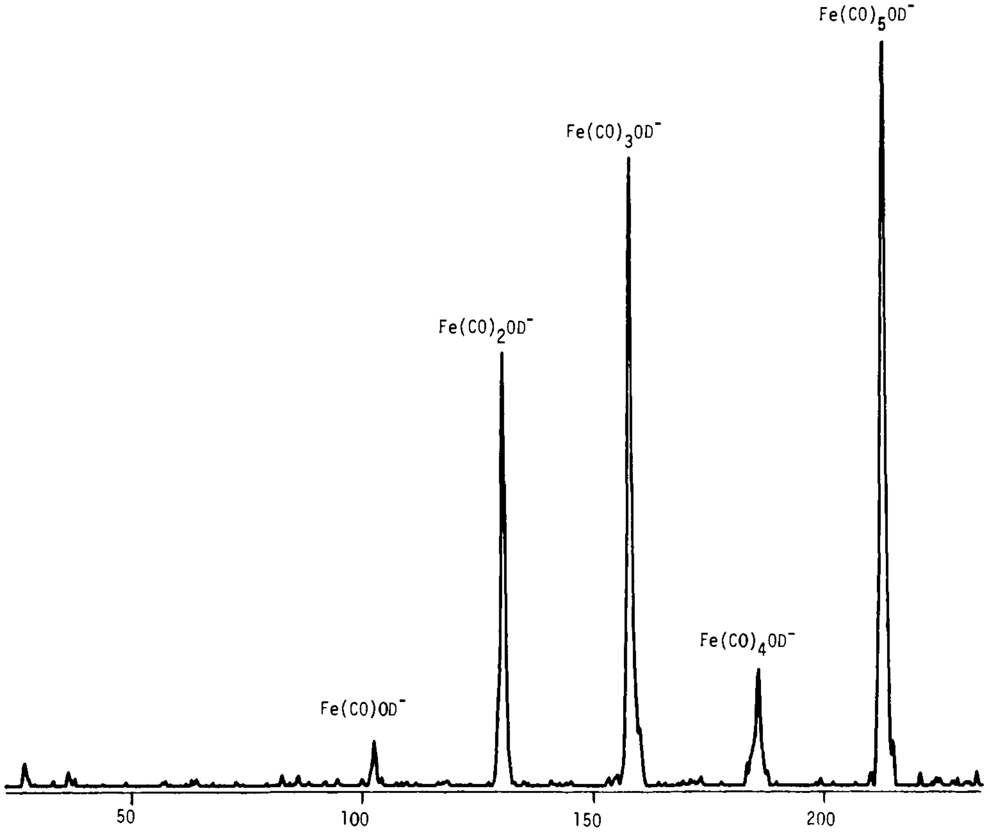

Figure 3. Collision-induced dissociation spectrum of Fe(CO)$_4$COOH$^-$. Ion axial kinetic energy approximately 20 eV; argon collision gas pressure ~2 mtorr. Fragmentation occurs by loss of CO ligands.

to exchange under these conditions. Our view of the mechanism for this somewhat unusual example of anionic gas-phase hydrogen–deuterium exchange[33] is shown for the CH_3COOD in Scheme II. Deuteration at the acyl oxygen of the metallocarboxylic acid anion produces an intermediate dihydroxy metal carbene which subsequently transfers the original proton back to acetate anion (A). Alternatively, a concerted mechanism involving a cyclic transition state can be envisaged (B). It is noteworthy in this regard that while the dibasic agent H_2S readily effects exchange with the deuterated ion **1**, CH_3SH does not, despite the nearly equal gas-phase acidities of these two species ($\Delta H_{acid}(H_2S) = 353.5$ kcal/mol; $\Delta H_{acid}(CH_3SH) = 359.0$ kcal/mol).[34]

Given a correct structural assignment for **3** as the iron carboxylic acid **1**, the foregoing results make possible several conclusions regarding its role in water-gas shift catalysis. On a millisecond time scale, isolated Fe(CO)$_4$COOH$^-$ is stable with respect to decarboxylation, despite the moderately favorable energetics; viz., a barrier exists. From the occurrence of reaction 8 for $n = 4$ we can conclude that ΔH_f(g) [(CO)$_4$FeCOOH$^-$] ≤ -256 kcal/mol.[31] Combining this with an estimate for ΔH_f(g) [(CO)$_4$FeH$^-$] $= -178 \pm 6$ kcal/mol[35] leads to a lower limit to the enthalpy of decarboxylation for **1** of approximately −17 kcal/mol. Since the measured rate of reaction 8 for $n = 4$ was large (Table I) it is reasonable to expect that reaction should also occur for $HO(H_2O)_5^-$. Therefore, the actual enthalpy of decarboxylation is likely to be significantly greater than −17 kcal/mol. Moreover, in the absence of a solvating medium, decarboxylation is not catalyzed by a single water molecule nor by stronger neutral bases such as amines since **3** sustains many hundreds of collisions with water in the course of its journey to the detector sampling orifice in our instrument and it appears to be totally unreactive in the presence of added $(CH_3)_2NH$. While we recognize that complete proton transfer from Fe(CO)$_4$COOH$^-$ to either H_2O or $(CH_3)_2NH$ is prohibitively endothermic without bulk solvation (ca. 100–150 kcal/mol), our results would seem to argue against a possible concerted mechanism for CO_2 loss wherein a hydrogen-bearing Lewis base assists proton delivery to the metal center (i.e., eq 12). The lack of even partial proton transfer from anionic acid to neutral base during a gas-phase encounter is further indicated by the failure of either H_2O or amines to effect H/D exchange in reactions with the deuterated ion **1**.

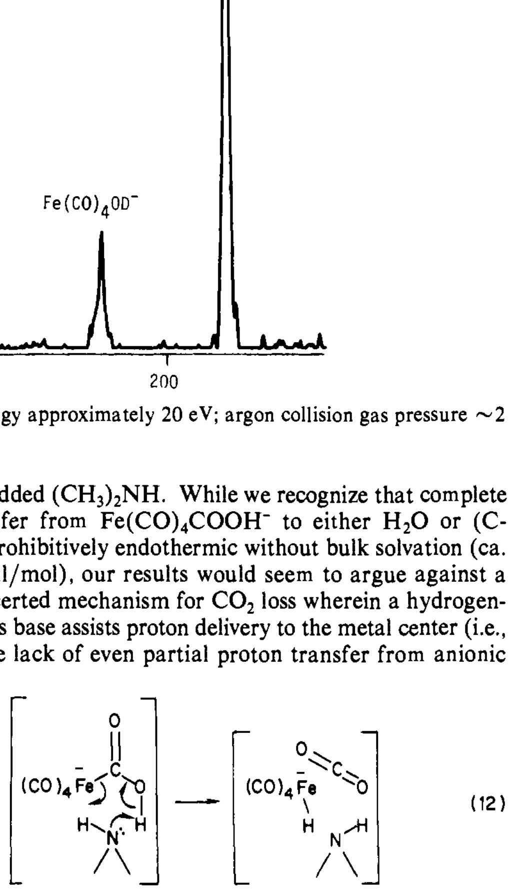

(12)

The collision-induced dissociation (CID) daughter ion spectrum of ion **3**, which we have obtained in our recently developed flowing afterglow-triple quadrupole apparatus,[16] is also supportive of obligatory base catalysis for decarboxylation. Fe(CO)$_4$COOH$^-$ undergoes fragmentation by *exclusive loss of CO* when subjected to low-energy CID (ca. 20 eV) under either single or multiple collision conditions (Figure 3). If decarboxylation of **3** were a thermal process, one might expect that deposition of excess internal energy by collisional activation in the gas phase would induce CO_2 loss. That no such fragmentation is observed suggests that the barrier to *decarboxylation* from an internally excited Fe(CO)$_4$COOH$^-$ ion exceeds that for *decarbonylation*.

We therefore conclude that Fe(CO)$_4$COOH$^-$ is a relatively stable species in the gas phase which exhibits no *intrinsic* propensity to lose CO_2 as depicted in eq 1. Furthermore, weak neutral bases alone do not promote ionization/decarboxylation of **3** as shown in eq 2 without benefit of solvation to support separated charges. The results of this investigation lend support to previous contentions[11,12] that decarboxylation of the Fe(CO)$_4$COOH$^-$ in-

---

(33) (a) Stewart, J. H.; Shapiro, R. H.; DePuy, C. H.; Bierbaum, V. M. *J. Am. Chem. Soc.* **1977**, *99*, 7650–7653. (b) Squires, R. R.; DePuy, C. H.; Bierbaum, V. M. *J. Am. Chem. Soc.* **1981**, *103*, 4256–4258.

(34) Bartmess, J. E.; McIver, R. T., Jr. In "Gas Phase Ion Chemistry"; Bowers, M. T., Ed.; Academic Press: New York, 1979; Vol. 2, Chapter 11.

(35) Based upon data taken from: Stevens, A. E.; Beauchamp, J. L., submitted for publication in *J. Am. Chem. Soc.*

termediate in the $Fe(CO)_5$-catalyzed WGSR proceeds via dianion **2** and requires base catalysis.

Note Added in Proof. While this manuscript was in press, two important developments have occurred. We recently found the hydroxide–*ammonia* cluster ion, $OH(NH_3)^-$, reacts with $Fe(CO)_5$ to yield, inter alia, $(CO)_4FeH^-$ as a primary product. Evidently, NH_3-catalyzed decarboxylation may occur within an ion–molecule complex such as that depicted in eq 12, provided excess internal energy from the initial OH^- attachment is available. Furthermore, a recent reinvestigation of $Fe(CO)_5$ in *nonaqueous* OH^- solutions has come to our attention which points to a protic solvent-catalyzed mechanism for $Fe(CO)_4COOH^-$ decarboxylation. We thank Professor P. C. Ford for stimulating discussion and a preprint of these results.

Acknowledgement is made to the donors of the Petroleum Research Fund, administered by the American Chemical Society, and to Research Corporation for the support of this research. We are especially grateful to T. Ridley for transforming our instrument blueprints into reality.

Registry No. 1, 90367-71-8; $Fc(CO)_5$, 13463-40-6; OH^-, 14280-30-9; $OH^-{\cdot}H_2O$, 23138-14-9; $OH^-{\cdot}2H_2O$, 34118-36-0; $OH^-{\cdot}3H_2O$, 34118-37-1; $OH{\cdot}4H_2O$, 24823-52-7.

Stereoselective Exchange Kinetics of L- and D-Histidines for Cl^- in the Interlayer of a Hydrotalcite-like Compound by the Chemical Relaxation Method

Tetsuya Ikeda, Hironori Amoh, and Tatsuya Yasunaga*

Contribution from the Department of Chemistry, Faculty of Science, Hiroshima University, Hiroshima 730, Japan. *Received January 30, 1984*

Abstract: The ion-exchange kinetics of L- and D-histidines for Cl^- in aqueous suspensions of Mg–hydrotalcite-like compound were studied by using the pressure-jump relaxation method with electric conductivity detection. Two relaxation phenomena were observed in both systems, and it was found that the difference in the L- and D-histidines as optical isomers appeared in both kinetic and static data. The fast relaxation was attributed to the release process of Cl^- in the interlayer induced by the histidine adsorption, while the slow relaxation was attributed to an intercalation process of histidine into the interlayer of the Mg–hydrotalcite-like compound. Kinetic and static parameters were determined and revealed differences between the ion-exchange properties of the L and D forms. The rate constants obtained for the D-histidine system were smaller than those for L-histidine, indicating a preference for that form. This result will give us a clue to understanding the origin of the chirality of living systems.

The stereoselective adsorption–desorption of molecules on clays may be related to the origin of chirality in living systems.[1-3] Several investigations have recently reported that clays preferentially adsorb one of the optical isomers. By studying the stereoselectivity of clays in the adsorption of optical isomers, we hoped that the role of clay minerals in chemical evolution might be clarified. However, the mechanism of adsorption–desorption of optical isomers has not been successfully determined because of the difficulties in studying these systems.

One of the interesting properties of layered compounds such as zeolite, montmorillonite, and hydrotalcite is their ability to selectively intercalate molecules into the interlayer regions.[4] This is particularly true for montmorillonite and hydrotalcite, which have shape-selective catalytic properties that can be changed by varying the interlayer distance. In previous papers,[5-10] ion-exchange and intercalation kinetics have been studied in zeolite, montmorillonite, and hydrotalcite aqueous systems. The results of these studies have confirmed the shape-selective properties of these clays for exchanging molecules.

In the present study, kinetic evidence is presented showing the preference of a Mg–hydrotalcite-like compound for a L-histidine isomer over a D-histidine isomer, in aqueous solutions. It is hoped that this study will provide important information with respect to the use of clays as catalysts for producing one of the optical isomers and the origin of asymmetry in biological systems.

Experimental Section

Kinetic measurements were carried out by using the pressure-jump apparatus with an electric conductivity detecting system. The details of the measurements of relaxation signals using the present apparatus and conductivity detection have been described elsewhere.[11] The time constant of the pressure jump is 80 μs.

The Mg–hydrotalcite-like compound ($Mg_{0.7}Al_{0.3}(OH)_2(CO_3)_{0.15}nH_2O$) was supplied from the Kyowa Chemical Co.[12] The chloride type of the Mg–hydrotalcite-like compound, Mg–HT(Cl), used was prepared by ion exchange of Cl^- for $CO_3{}^{2-}$ in Mg–HT(CO_3) and was washed several times with distilled water. The anion-exchange capacity was determined to be 100 mequiv/100 g from the OH^- titration. The Mg–HT(Cl) particles were dispersed in aqueous solution by ultrasonication and formed very stable suspensions under the present experimental condition. Microscopic examination confirmed that the mean diameter of the Mg–HT(Cl) particles is less than 1 μm.

The amounts of L- and D-histidines adsorbed were determined indirectly from the concentration change in the supernatant solution by means of the colorimetric ninhydrin method at a wavelength of 570 nm. Before the measurements, samples of the Mg–HT(Cl) suspensions containing L- and D-histidines were centrifuged for 40 min at 20000*g* in order to settle the particles completely. The concentrations of H^+ and Cl^- were determined with a glass electrode and a Cl electrode, respectively.

---

(1) Kachalski, A. *Nature (London)* **1970**, *228*, 636.
(2) Degens, E. T.; Matheja, J.; Jackson, T. A. *Nature (London)* **1970**, *227*, 492.
(3) Yamagishi, A. *J. Phys. Chem.* **1982**, *86*, 2472.
(4) "Intercalation Chemistry"; Whittingham, M. S., Jacobson, A. J., Eds.; Academic Press: New York, 1982.
(5) Ikeda, T.; Sasaki, M.; Yasunaga, T. *J. Phys. Chem.* **1983**, *87*, 745.
(6) Ikeda, T.; Sasaki, M.; Yasunaga, T. *J. Phys. Chem.* **1982**, *86*, 1680.
(7) Ikeda, T.; Nakahara, J.; Sasaki, M.; Yasunaga, T. *J. Colloid Interface Sci.* **1984**, *97*, 278.
(8) Ikeda, T.; Sasaki, M.; Yasunaga, T. *J. Colloid Interface Sci.* **1984**, *98*, 192.
(9) Ikeda, T.; Yasunaga, T. *J. Colloid Interface Sci.* **1984**, *99*, 183.
(10) Ikeda, T.; Yasunaga, T. *J. Phys. Chem.* **1984**, *88*, 1253.
(11) Hachiya, K.; Ashida, M.; Sasaki, M.; Kan, H.; Inoue, T.; Yasunaga, T. *J. Phys. Chem.* **1979**, *83*, 1866.
(12) Miyata, S. *Clays Clay Miner.* **1975**, *23*, 369.

0002-7863/84/1506-5772$01.50/0